Synthesis and Characterization of Several Dicopper(I) Complexes and a Spin-Delocalized Dicopper(I,II) Mixed-Valence Complex Using a 1,8-Naphthyridine-Based Dinucleating Ligand

Chuan He and Stephen J. Lippard*

Department of Chemistry, Massachusetts Institute of Technology, Cambridge, Massachusetts 02139

The synthesis of dicopper(I) complexes [Cu$_2$(BBAN)(MeCN)$_2$](OTf)$_2$ (**1**), [Cu$_2$(BBAN)(py)$_2$](OTf)$_2$ (**2**), [Cu$_2$(BBAN)(1-Me-BzIm)$_2$](OTf)$_2$ (**3**), [Cu$_2$(BBAN)(1-Me-Im)$_2$](OTf)$_2$ (**4**), and [Cu$_2$(BBAN)(μ-O$_2$CCPh$_3$)](OTf) (**5**), where BBAN = 2,7-bis((dibenzylamino)methyl)-1,8-naphthyridine, py = pyridine, 1-Me-Im = 1-methylimidazole, and 1-Me-BzIm = 1-methylbenzimidazole, are described. Short copper−copper distances ranging from 2.6151(6) to 2.7325(5) Å were observed in the solid-state structures of these complexes depending on the terminal ligands used. The cyclic voltammogram of compound **5** dissolved in THF exhibited a reversible redox wave at $E_{1/2}$ = −25 mV vs Cp$_2$Fe$^+$/Cp$_2$Fe. When complex **5** was treated with 1 equiv of silver(I) triflate, a mixed-valence dicopper(I,II) complex [Cu$_2$(BBAN)(μ-O$_2$CCPh$_3$)(OTf)](OTf) (**6**) was prepared. A short copper−copper distance of 2.4493(14) Å observed from the solid-state structure indicates the presence of a copper−copper interaction. Variable-temperature EPR studies showed that complex **6** has a fully delocalized electronic structure in frozen 2-methyltetrahydrofuran solution down to liquid helium temperature. The presence of anionic ligands seems to be an important factor to stabilize the mixed-valence dicopper(I,II) state. Compounds **1**−**4** with neutral nitrogen-donor terminal ligands cannot be oxidized to the mixed-valence analogues either chemically or electrochemically.

Introduction

Copper is used widely as a metal cofactor to perform different functions in biology. One example is the spin-delocalized dinuclear mixed-valence copper(I,II) cluster identified in the Cu$_A$ site of cytochrome *c* oxidase (CcO) and nitrous oxide reductase (N$_2$OR), which mediates electron transfer. X-ray crystallographic studies on the Cu$_A$ sites in CcO and N$_2$OR revealed short copper−copper distances ($\sim$2.5 Å) indicative of metal−metal bonding.[1−4] The presence of such metal−metal interactions was previously unprecedented in biological systems. The unpaired spin in the Cu$_A$ site is fully delocalized over two copper ions,[5,6] as revealed by an EPR signal with seven-line hyperfine coupling patterns arising from spin interactions with both I = 3/2 copper ions.[7,8]

Fully delocalized, type III mixed-valence copper complexes such as the Cu$_A$ site are rare in inorganic chemistry. Most mixed-valence dicopper complexes belong to class I with the unpaired spin fully localized on one metal center.[9] The small number of class II, mixed-valence dicopper compounds usually exhibit temperature-dependent spin exchange phenomena. The unpaired spin is trapped at low temperature, as indicated by EPR spectroscopy for these systems.[10,11] Type III mixed-valence dicopper(I,II) complexes have unpaired spin delocalized over two copper centers even at liquid-helium temperature.

To date three types of class III dicopper complexes have been prepared that reproduce features of the fully delocalized mixed-valence Cu$_A$ site (Table 1). A tridentate N$_2$S ligand was used to assemble a bis(μ-thiolato)dicopper(I,II) compound, where the unpaired electron was fully delocalized over two copper atoms.[12,13] The Cu−Cu separation of 2.9306(9) Å in the structure of this compound is long compared to the short Cu−Cu distance of 2.5 Å in the Cu$_A$ center. An irreversible one-electron reduction or oxidation wave was recorded at $E_{1/2}$ = +350 mV vs SCE for this complex in methanol. Several class III delocalized mixed-valence dicopper compounds with short Cu−Cu distances of 2.415(1), 2.419(1), and 2.448(1) Å were synthesized using octaazacryptand macrobicyclic ligands.[14−16] A reversible redox potential of +310 mV vs Ag/AgCl in DMF

(1) Iwata, S.; Ostermeier, C.; Ludwig, B.; Michel, H. *Nature* **1995**, *376*, 660−669.
(2) Tsukihara, T.; Aoyama, H.; Yamashita, E.; Tomizaki, T.; Yamaguchi, H.; Shinzawa-Itoh, K.; Nakashima, R.; Yaono, R.; Yoshikawa, S. *Science* **1995**, *269*, 1069−1074.
(3) Tsukihara, T.; Aoyama, H.; Yamashita, E.; Tomizaki, T.; Yamaguchi, H.; Shinzawa-Itoh, K.; Nakashima, R.; Yaono, R.; Yoshikawa, S. *Science* **1996**, *272*, 1136−1144.
(4) Brown, K.; Tegoni, M.; Prudêncio, M.; Pereira, A. S.; Besson, S.; Moura, J. J.; Moura, I.; Cambillau, C. *Nat. Struct. Biol.* **2000**, *7*, 191−195.
(5) Farrar, J. A.; Neese, F.; Lappalainen, P.; Kroneck, P. M. H.; Saraste, M.; Zumft, W. G.; Thomson, A. J. *J. Am. Chem. Soc.* **1996**, *118*, 11501−11514.
(6) Gamelin, D. R.; Randall, D. W.; Hay, M. T.; Houser, R. P.; Mulder, T. C.; Canters, G. W.; de Vries, S.; Tolman, W. B.; Lu, Y.; Solomon, E. I. *J. Am. Chem. Soc.* **1998**, *120*, 5246−5263.
(7) Neese, F.; Zumft, W. G.; Antholine, W. E.; Kroneck, P. M. H. *J. Am. Chem. Soc.* **1996**, *118*, 8692−8699.
(8) Lappalainen, P.; Aasa, R.; Malmström, B. G.; Saraste, M. *J. Biol. Chem.* **1993**, *268*, 26416−26421.
(9) Dunaj-Jurco, M.; Ondrejovic, G.; Melnik, M.; Garaj, J. *Coord. Chem. Rev.* **1988**, *83*, 1−28.
(10) Long, R. C.; Hendrickson, D. N. *J. Am. Chem. Soc.* **1983**, *105*, 1513−1521.
(11) Gagné, R. R.; Koval, C. A.; Smith, T. J.; Cimolino, M. C. *J. Am. Chem. Soc.* **1979**, *101*, 4571−4580.
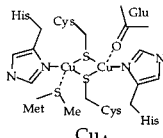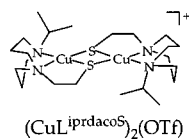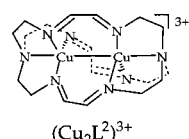(12) Houser, R. P.; Young, V. G., Jr.; Tolman, W. B. *J Am. Chem. Soc.* **1996**, *118*, 2101−2102.
(13) Abbreviations: L^{iPrdacoS} = 1-isopropyl-5-(ethylthiolato)-1,5-diazocyclooctane; L^2 = N(CH$_2$CH$_2$N=CHCH=NCH$_2$CH$_2$)$_3$N.
(14) Harding, C.; Nelson, J.; Symons, M. C. R.; Wyatt, J. *J. Chem. Soc., Chem. Commun.* **1994**, 2499−2500.
(15) Harding, C.; McKee, V.; Nelson, J. *J. Am. Chem. Soc.* **1991**, *113*, 9684−9685.
(16) Barr, M. E.; Smith, P. H.; Antholine, W. E.; Spencer, B. *J. Chem. Soc., Chem. Commun.* **1993**, 1649−1652.
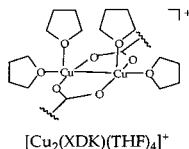
Table 1. Structural, Spectroscopic, and Electrochemical Data for Selected Examples of Class III Mixed-Valence Dicopper Complexes

Complex	UV-vis-NIR (λ_{max}, nm (ε, M^{-1} cm^{-1}))	Cu-Cu dist (Å)	EPR[c]	$E_{1/2}$ (mV)	ref
Cu_A	363 (1200), 480 (3000), 532 (3000), 808 (1600)	2.5-2.7	$g_{min} = 2.003$, $g_{mid} = 2.005$, $g_{max} = 2.203$, $A_x^{65\text{-}Cu} = 105$ G, $A_y^{65\text{-}Cu} = 116$ G, $A_z^{65\text{-}Cu} = 235$ G,	~ +240[d] ~ -560[e]	1-8, 10, 11 32
$(CuL^{iprdacoS})_2(OTf)$	358 (2700), 602 (800), 786 (sh), 1466 (1200)	2.9306(9)	$g_1 = 2.010$, $g_2 = 2.046$, $g_3 = 2.204$, $A_2^{Cu} = 36.3$ G, $A_3^{Cu} = 49.9$ G		12
$(Cu_2L^2)^{3+}$	600-650 (1500-3500)[a], 750-780 (5000)	2.448[b]	$g_{||} = 2.004$, $g_{\perp} = 2.148$, $A_{||} = 11$ G, $A_{\perp} = 111$ G	+310[f] -206[e]	14,15
$[Cu_2(XDK)(THF)_4]^+$	536 (1600), 923 (1200)	2.4246(12)	$g_1 = 2.030$, $g_2 = 2.158$, $g_3 = 2.312$, $A_1^{Cu} = 20.0$ G, $A_2^{Cu} = 55.0$ G, $A_3^{Cu} = 122.5$ G	-218[e]	17,18
6	500 (1583), 550 (1425), 660 (1450), 875 (3775)	2.4500(15)	$g_1 = 2.002$, $g_2 = 2.100$, $g_3 = 2.222$, $A_1^{Cu} = 30.0$ G, $A_2^{Cu} = 60.0$ G, $A_3^{Cu} = 143.0$ G	-25[e]	this work

[a] Only ranges were reported for the absorption maxima and molar absorptivities. [b] No esd reported. [c] All parameters were derived from simulated spectra. [d] Potential vs NHE. [e] Potential vs Cp_2Fe^+/Cp_2Fe in THF. [f] Potential vs Ag/AgCl in DMF. See ref 18 for scaling literature potentials to potentials vs Cp_2Fe^+/Cp_2Fe in THF.

(−206 mV vs Cp_2Fe^+/Cp_2Fe in THF) was reported for one of these compounds.[15] The third example of class III delocalized mixed-valence Cu(1.5)−Cu(1.5) compounds comes from our laboratory. These species were assembled by using the convergent bis(carboxylate) ligand, *m*-xylylenediamine bis(Kemp's triacid imide) (H₂XDK).[17,18] The metal−metal distances in these dicopper(I,II) XDK complexes are ∼2.4 Å, and a reversible redox couple with $E_{1/2}$ of −218 mV vs Cp_2Fe^+/Cp_2Fe in THF was observed for one of them.[18]

The reversible redox potentials recorded for two families of class III mixed-valence dicopper complexes are very close to each other when converted to same scale (Table 1), even though very different ligand sets were used. The negatively charged carboxylate groups in the all-oxygen bis(carboxylate) complex do not lower the redox potential of the system compared to the neutral all-nitrogen ligands available in the octaazacryptand compound. More experimental details are required, however, before any generalizations can be made about this and other properties of the fully delocalized dicopper(I,II) mixed-valence system. In the present study we have prepared a class III mixed-valence dicopper complex containing both nitrogen and oxygen donor ligands. The physical properties of this complex were investigated, with special attention paid to the redox potentials,
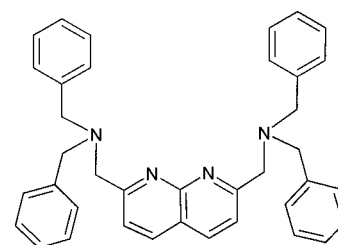
BBAN

Figure 1. Schematic representation of BBAN.

and compared with previous examples to help elucidate further the nature of their mixed-valence-character.

2,7-Bis((dibenzylamino)methyl)-1,8-naphthyridine (BBAN) (Figure 1) was employed as the tetradentate dinucleating ligand in this work. The 1,8-naphthyridine ligand scaffold affords short metal−metal distances, as reported previously.[19−21] A series of dicopper(I) compounds $[Cu_2(BBAN)(MeCN)_2](OTf)_2$ (**1**), $[Cu_2(BBAN)(py)_2](OTf)_2$ (**2**), $[Cu_2(BBAN)(1\text{-Me-BzIm})_2]$-$(OTf)_2$ (**3**), $[Cu_2(BBAN)(1\text{-Me-Im})_2](OTf)_2$ (**4**), and $[Cu_2(BBAN)$-

(17) LeCloux, D. D.; Davydov, R.; Lippard, S. J. *J. Am. Chem. Soc.* **1998**, *120*, 6810−6811.

(18) LeCloux, D. D.; Davydov, R.; Lippard, S. J. *Inorg. Chem.* **1998**, *37*, 6814−6826.

(19) Tikkanen, W. R.; Krüger, C.; Bomben, K. D.; Jolly, W. L.; Kaska, W. C.; Ford, P. C. *Inorg. Chem.* **1984**, *23*, 3633−3638.

(20) Boelrijk, A. E. M.; Neenan, T. X.; Reedijk, J. *J. Chem. Soc., Dalton Trans.* **1997**, 4561−4570.

(21) He, C.; Lippard, S. J. *J. Am. Chem. Soc.* **2000**, *122*, 184−185.

(μ-O$_2$CCPh$_3$)](OTf) (**5**), where py = pyridine, 1-Me-Im = 1-methylimidazole, and 1-Me-BzIm = 1-methylbenzimidazole, were prepared and their chemical and electrochemical oxidations investigated. A mixed-valence complex [Cu$_2$(BBAN)-(μ-O$_2$CCPh$_3$)(OTf)](OTf) (**6**) was obtained when complex **5** was treated with 1 equiv of silver(I) triflate. The physical properties of complex **6** were studied and compared with those of previous compounds.

Experimental Section

General Procedures and Methods. All reagents were obtained from commercial suppliers and used without further purification unless otherwise noted. THF was distilled from sodium benzophenone ketyl under nitrogen. Pentane and Et$_2$O were purified by passing through activated Al$_2$O$_3$ columns under nitrogen. Dichloromethane was distilled from CaH$_2$ under nitrogen. Fourier transform infrared spectra were recorded on a Bio-Rad FTS135 instrument. UV−vis spectra were recorded on a Varian 1-E spectrophotometer. The ligand BBAN was synthesized according to procedures reported elsewhere.[22] [Cu(CH$_3$-CN)$_4$](OTf) was prepared by following a known procedure.[23] All air-sensitive manipulations were carried out either in a nitrogen-filled Vacuum Atmospheres drybox or by standard Schlenk line techniques.

Electrochemistry. Cyclic voltammetric measurements were performed in a Vacuum Atmospheres drybox under N$_2$ with an EG&G model 263 potentiostat. A three-electrode configuration consisting of a 1.75 mm^2 platinum working electrode, a Ag/AgNO$_3$ (0.1 M in CH$_3$-CN) reference electrode, and a coiled platinum wire auxiliary electrode was used. The supporting electrolyte was 0.5 M (Bu$_4$N)(PF$_6$). Sample concentrations of 2 mM were used for typical experiments. Scan rate profiles were conducted for each sample, at scan speeds of 25−150 mV/s, and compared to that obtained for Cp$_2$Fe under identical conditions. All cyclic voltammograms were externally referenced to Cp$_2$Fe.

EPR Spectroscopy. The EPR spectrum was collected as frozen 2-methyltetrahydrofuran glass on a Bruker model 300 ESP X-band spectrometer operating at 9.37 GHz and running WinEPR software. Low temperature was maintained at 77 K with a specially designed coldfinger filled with liquid N$_2$ and at liquid-helium temperature with an Oxford Instruments EPR 900 crystat. Simulation was carried out with the WINEPR SimFonia program package.[24] Simultaneous coupling of the unpaired spin to two $I = 3/2$ copper centers was incorporated into the fit.

[Cu$_2$(BBAN)(CH$_3$CN)$_2$](OTf)$_2$ (1). A portion of BBAN (50 mg, 0.091 mmol) in THF (0.5 mL) was added to a solution of [Cu(CH$_3$-CN)$_4$](OTf) (68.7 mg, 0.182 mmol) in THF (1 mL). The solution turned pink, and the product began to precipitate. After 1 h of stirring, the pink product was isolated and dried under vacuum (80.5 mg, 84%). Single crystals suitable for X-ray crystallographic study were obtained by diffusion of Et$_2$O into a saturated CH$_2$Cl$_2$ solution at −30 °C. ^{1}H NMR (CDCl$_3$, 300 MHz): δ 2.17 (s, 6 H), 4.13 (s, 8 H), 4.22 (s, 4 H), 7.10−7.26 (m, 12 H), 7.32−7.50 (m, 8 H), 7.62 (broad, 2 H), 8.26 (d, $J = 8$ Hz, 2 H). FTIR (KBr, cm^{-1}): 3085 (w), 3064 (w), 3032 (w), 2932 (w), 2859 (w), 2290 (w), 1610 (m), 1560 (w), 1264 (s), 1226 (m), 1152 (s), 1032 (s), 877 (w), 852 (w), 791 (w), 754 (m), 706 (m), 638 (s). Anal. Calcd for **1**, C$_{44}$H$_{42}$N$_6$O$_6$S$_2$F$_6$Cu$_2$: C, 50.04; H, 4.01; N, 7.96. Found: C, 49.86; H, 4.20; N, 7.81.

[Cu$_2$(BBAN)(py)$_2$](OTf)$_2$ (2). A portion of BBAN (50 mg, 0.091 mmol) in THF (0.5 mL) was added to a solution of [Cu(CH$_3$CN)$_4$]-(OTf) (68.7 mg, 0.182 mmol) in THF (1 mL). The color of the solution turned pink. A portion of pyridine (15 μL, 0.182 mmol) was added, and the solution turned yellow. After 30 min of stirring, the solvent was removed under vacuum. The residue was dissolved in CH$_2$Cl$_2$. Crystallization by vapor diffusion of Et$_2$O into this CH$_2$Cl$_2$ solution yielded green-brown blocks suitable for X-ray crystallography (78 mg, 76%). ^{1}H NMR (CDCl$_3$, 300 MHz): δ 3.76 (s, 8 H), 4.43 (s, 4 H),

7.14−7.40 (m, 22 H), 7.46 (d, $J = 7$ Hz, 2 H), 7.63 (d, $J = 7$ Hz, 2 H), 7.66−7.80 (m, 2 H), 8.11 (d, $J = 7$ Hz, 2 H), 8.80 (d, $J = 4$ Hz, 4 H). FTIR (KBr, cm^{-1}): 3072 (m), 3029 (w), 2929 (w), 2862 (w), 2839 (w), 1666 (s), 1519 (m), 1498 (m), 1488 (m), 1449 (s), 1436 (m), 1353 (w), 1282 (s), 1222 (m), 1153 (s), 1069 (w), 1029 (s), 971 (m), 879 (m), 856 (m), 788 (m), 755 (s), 700 (s), 630(s). Anal. Calcd for **2**, C$_{50}$H$_{46}$N$_6$O$_6$S$_2$F$_6$Cu$_2$: C, 53.04; H, 4.10; N, 7.42. Found: C, 52.93; H, 3.91; N, 7.24.

[Cu$_2$(BBAN)(1-Me-BzIm)$_2$](OTf)$_2$ (3). A portion of BBAN (30 mg, 0.055 mmol) in THF (0.5 mL) was added to a solution of [Cu(CH$_3$-CN)$_4$](OTf) (41.2 mg, 0.11 mmol) in THF (1 mL). The color of the solution turned to pink. A portion of 1-methylbenzimidazole (14.4 mg, 0.11 mmol) was added, and the solution turned yellow. After 30 min of stirring, the solvent was removed under vacuum. The residue was dissolved in CH$_2$Cl$_2$. Purple blocks suitable for X-ray crystallography were obtained by vapor diffusion of Et$_2$O into the CH$_2$Cl$_2$ solution. The product became a blue powder after collection and drying under vacuum (32 mg, 47%). ^{1}H NMR (CDCl$_3$, 300 MHz): δ 3.54−4.00 (m, broad, 14 H), 4.45 (s, broad, 4 H), 7.08 ∼ 7.46 (m, 24 H), 7.63 (d, $J = 8$ Hz, 2 H), 7.89 (d, $J = 7.8$ Hz, 2 H), 8.11 (d, $J = 7$ Hz, 2 H), 8.92 (s, 2 H). FTIR (KBr, cm^{-1}): 3110 (m), 3087 (w), 3062 (m), 3030 (m), 2927 (w), 2891 (w), 2853 (m), 1607 (s), 1523 (s), 1477 (w), 1459 (s), 1369 (m), 1277 (s), 1224 (m), 1153 (s), 1070 (w), 1030 (s), 974 (w), 877 (w), 856 (w), 747 (s), 703 (s), 638 (s). Anal. Calcd for **3**, C$_{56}$H$_{52}$N$_8$O$_6$S$_2$F$_6$Cu$_2$: C, 54.32; H, 4.23; N, 9.05. Found: C, 54.02; H, 4.33; N, 8.96.

[Cu$_2$(BBAN)(1-Me-Im)$_2$](OTf)$_2$ (4). A portion of BBAN (20 mg, 0.036 mmol) in THF (0.5 mL) was added to a solution of [Cu(CH$_3$-CN)$_4$](OTf) (27.5 mg, 0.073 mmol) in THF (1 mL). The color of the solution turned to pink. A portion of 1-methylimidazole (5.8 μL, 0.073 mmol) was added, and the solution turned yellow. After 30 min of stirring, the solvent was removed under vacuum. The residue was dissolved in CH$_2$Cl$_2$. Layering Et$_2$O on top of the CH$_2$Cl$_2$ solution for 1 week yielded green blocks suitable for X-ray crystallography (19 mg, 46%). ^{1}H NMR (CDCl$_3$, 300 MHz): δ 3.78 (s, 8 H), 3.84 (s, 6 H), 4.24 (s, 4 H), 6.90−6.98 (broad, 2 H), 7.08−7.48 (m, broad, 20 H), 7.56−7.72 (m, broad, 4 H), 8.23 (broad, 2 H), 8.37 (d, $J = 7$ Hz, 2 H). FTIR (KBr, cm^{-1}): 3136 (m), 3126 (w), 3132 (w), 3062 (w), 2962 (w), 2843 (w), 1608 (s), 1541 (m), 1522 (m), 1497 (w), 1458 (m), 1427 (m), 1368 (w), 1264 (m), 1224 (m), 1160 (s), 1114 (m), 1099 (w), 1029 (s), 970 (w), 857 (w), 819 (w), 791 (w), 749 (s), 703 (m), 657 (m), 638 (s). Anal. Calcd for **4**, C$_{52}$H$_{40}$N$_8$O$_6$S$_2$F$_6$Cu$_2$: C, 50.65; H, 4.25; N, 9.85. Found: C, 50.27; H, 4.10; N, 9.77.

[Cu$_2$(BBAN)(μ-O$_2$CCPh$_3$)](OTf) (5). A portion of BBAN (20 mg, 0.036 mmol) in THF (0.5 mL) was added to a solution of [Cu(CH$_3$-CN)$_4$](OTf) (27.5 mg, 0.073 mmol) in THF (1 mL). The solution turned pink, and a solution of sodium triphenylacetate (11.3 mg, 0.036 mmol) in THF (0.5 mL) was added. The color of the solution turned to green. After 30 min of stirring, the solvent was removed under vacuum. Green plates suitable for X-ray crystallography were obtained from pentane/Et$_2$O/benzene (27 mg, 67%). ^{1}H NMR (CDCl$_3$, 300 MHz): δ 3.70−4.30 (m, broad, 12 H), 7.00−7.46 (m, 29 H), 7.58−7.70 (m, 6 H), 8.40 (broad, 2 H), 8.57 (broad, 2 H), 7.62 (broad, 2 H), 8.26 (d, $J = 8$ Hz, 2 H). FTIR (KBr, cm^{-1}): 3080 (m), 3032 (m), 2920 (m), 2848 (w), 1617 (s), 1606 (s), 1551 (s), 1494 (m), 1479 (s), 1448 (m), 1380 (s), 1274 (s), 1268 (s), 1224 (m), 1161 (s), 1149 (s), 1031 (s), 998 (s), 873 (s), 755 (s), 743 (s), 701 (s), 638 (s). UV−vis (THF, λ_{max}, nm (ϵ, M^{-1} cm^{-1})): 640 (96). Anal. Calcd for **5**, C$_{59}$H$_{51}$N$_4$O$_5$SF$_3$Cu$_2$: C, 63.71; H, 4.62; N, 5.04. Found: C, 63.59; H, 4.45; N, 4.96.

[Cu$_2$(BBAN)(μ-O$_2$CCPh$_3$)(OTf)](OTf) (6). A portion of BBAN (20 mg, 0.036 mmol) in THF (0.5 mL) was added to a solution of [Cu-(CH$_3$CN)$_4$](OTf) (27.5 mg, 0.073 mmol) in THF (1 mL). The solution turned pink, and a solution of sodium triphenylacetate (11.3 mg, 0.036 mmol) in THF (0.5 mL) was added. The color of the solution turned to yellow. After 30 min of stirring, a solution of AgOTf (9.4 mg, 0.036 mmol) in THF (0.5 mL) was added. The mixture was allowed to stir for 5 h. Solvent was removed under vacuum. The residue was extracted with CH$_2$Cl$_2$ and filtered. Deep purple plates suitable for X-ray crystallography were obtained from pentane/Et$_2$O/CH$_2$Cl$_2$ (11 mg, 24%). FTIR (KBr, cm^{-1}): 3085 (w), 3065 (m), 3031 (w), 2940 (w), 2920 (w), 2871 (w), 1616 (s), 1604 (m), 1541 (m), 1496 (m), 1458 (m),

(22) He, C.; Lippard, S. J. *Tetrahedron* **2000**, *56*, 8245−8252.
(23) Kubas, G. J. *Inorg. Synth.* **1979**, *19*, 90−92.
(24) *WINEPR-SimFonia, 1.25*; Bruker Analytik GmbH: Karlsruhe, FRG, 1994−1996.

Table 2. Summary of X-ray Crystallographic Data

	1·2CH$_2$Cl$_2$	**2**	**3·CH$_2$Cl$_2$**	**4·Et$_2$O**	**5·1.5C$_6$H$_6$**	**6·CH$_2$Cl$_2$**
formula	C$_{46}$H$_{46}$N$_6$O$_6$ Cl$_4$F$_6$S$_2$Cu$_2$	C$_{50}$H$_{46}$N$_6$O$_6$ F$_6$S$_2$Cu$_2$	C$_{57}$H$_{54}$N$_8$O$_6$ Cl$_2$F$_6$S$_2$Cu$_2$	C$_{52}$H$_{58}$N$_8$O$_7$ F$_6$S$_2$Cu$_2$	C$_{68}$H$_{60}$N$_4$O$_5$ F$_3$Scu$_2$	C$_{60.50}$H$_{52}$N$_4$O$_8$ ClF$_6$S$_2$Cu$_2$
fw	1225.89	1132.13	1323.18	1212.26	1229.34	1303.71
space group	$C2/c$	$C2/c$	P1	P1	$C2/c$	$P2_1/c$
a, Å	16.9286(3)	15.490(5)	12.8261(5)	11.8651(2)	41.2217(10)	22.5642(2)
b, Å	15.9582(1)	15.846(5)	15.0676(6)	12.5037(2)	13.9946(4)	22.3852(4)
c, Å	21.2111(3)	21.070(5)	16.2679(6)	20.9961(4)	20.7004(6)	23.5102(4)
α, deg			85.8140(10)	72.8750(10)		
β, deg	111.5570(10)	101.369(5)	83.8290(10)	88.5070(10)	102.3350(10)	95.5300(10)
γ, deg			69.9740(10)	68.7790(10)		
V, Å^3	5329.36(13)	5070(3)	2934.5(2)	2763.62(8)	11 666.0(6)	11819.8(3)
Z	4	4	2	2	8	8
T, °C	−85	−85	−85	−85	−85	85
ρ_{calcd}, g cm^{-3}	1.528	1.483	1.497	1.457	1.400	1.465
μ(Mo Kα), mm^{-1}	1.150	0.998	0.963	0.923	0.830	0.912
R^b	0.0447	0.0326	0.0533	0.0443	0.0571	0.0743
wR2^c	0.1261	0.0971	0.1615	0.1259	0.1558	0.1751

^{a} Observation criterion: $I > 2\sigma(I)$. ^{b} R = $\Sigma||F_o| - |F_c||/\Sigma|F_o|$. ^{c} wR2 = $\{\Sigma[w(F_o{}^2 - F_c{}^2)^2]/\Sigma[w(F_o{}^2)^2]\}^{1/2}$.

1450 (m), 1397 (s), 1274 (s), 1235 (s), 1219 (s), 1160 (s), 1150 (s), 1296 (s), 1025 (s), 917 (w), 881 (w), 850 (w), 815 (w), 789 (w), 749 (s), 700 (s), 637 (s). UV−vis (THF, λ_{max}, nm (ϵ, M^{-1} cm^{-1})): 875 (3775), 660 (1450), 550 (1425), 500 (1583). Anal. Calcd for **6**, C$_{60}$H$_{51}$N$_4$O$_8$S$_2$F$_6$Cu$_2$: C, 57.14; H, 4.08; N, 4.44. Found: C, 56.86; H, 4.24; N, 4.28.

Collection and Reduction of X-ray Data. X-ray crystallographic studies (Table 2) were carried out on a Bruker CCD diffractometer with graphite-monochromatized Mo Kα radiation (λ = 0.710 73 Å) controlled by a Pentium-based PC running the SMART software package.[25] Single crystals were mounted at room temperature on the ends of quartz fibers in Paratone N oil and data were collected at 193 K in a stream of cold N$_2$ maintained by a Bruker LT-2A nitrogen cryostat. Data collection and reduction protocols are described in detail elsewhere.[26] The structures were solved by direct methods and refined on F^2 by using the SHELXTL software package.[27] Empirical absorption corrections were applied by using the SADABS program.[28] Structures were checked for higher symmetry with the PLATON program.[29] All non-hydrogen atoms were refined anisotropically. Hydrogen atoms were assigned idealized locations and given an isotropic thermal parameter 1.2 times the thermal parameter of the carbon atom to which they were attached.

In the structure of **3**, one chlorine atom of a solvent dichloromethane was disordered over three positions, Cl(1), Cl(1A), and Cl(1B), refined at occupancies of 0.4, 0.3, and 0.3, respectively. The other chlorine atom was also disordered over three positions, Cl(2), Cl(2A), and Cl(2B), refined at occupancies of 0.5, 0.4, and 0.1, respectively. In the structure of **5**, the carbon and fluorine atoms of the triflate molecule were disordered over two sets of positions, C(59), F(1), F(2), and F(3) and C(59B), F(1B), F(2B), and F(3B), refined at occupancies of 0.6 and 0.4, respectively. Two asymmetric units share a solvent benzene molecule. This benzene molecule was also disordered over two sets of positions, C(7sA), C(8sA), and C(9sA) and C(7sB), C(8sB), and C(9sB), respectively, each refined at half-occupancy.

Results and Discussion

Preparation and Structural Characterization of Dicopper(I) Complexes: [Cu$_2$(BBAN)L$_2$](OTf)$_2$, L = MeCN (1), py (2), 1-Me-BzIm (3), and 1-Me-Im (4); [Cu$_2$(BBAN)- (μ-O$_2$CCPh$_3$)](OTf) (5). Dicopper(I) complexes of BBAN with

(25) *SMART v5.05*; Bruker AXS: Madison, WI, 1998.
(26) Feig, A. L.; Bautista, M. T.; Lippard, S. J. *Inorg. Chem.* **1996**, *25*, 6892−6898.
(27) Sheldrick, G. M. *SHELXTL97-2: Program for the Refinement of Crystal Structures*; University of Göttingen: Göttingen, Germany, 1997.
(28) Sheldrick, G. M. *SADABS: Area-Detector Absorption Correction*; University of Göttingen: Göttingen, Germany, 1996.
(29) Spek, A. L. *PLATON, A Multipurpose Crystallographic Tool*; Utrecht University: Utrecht, The Netherlands, 1998.
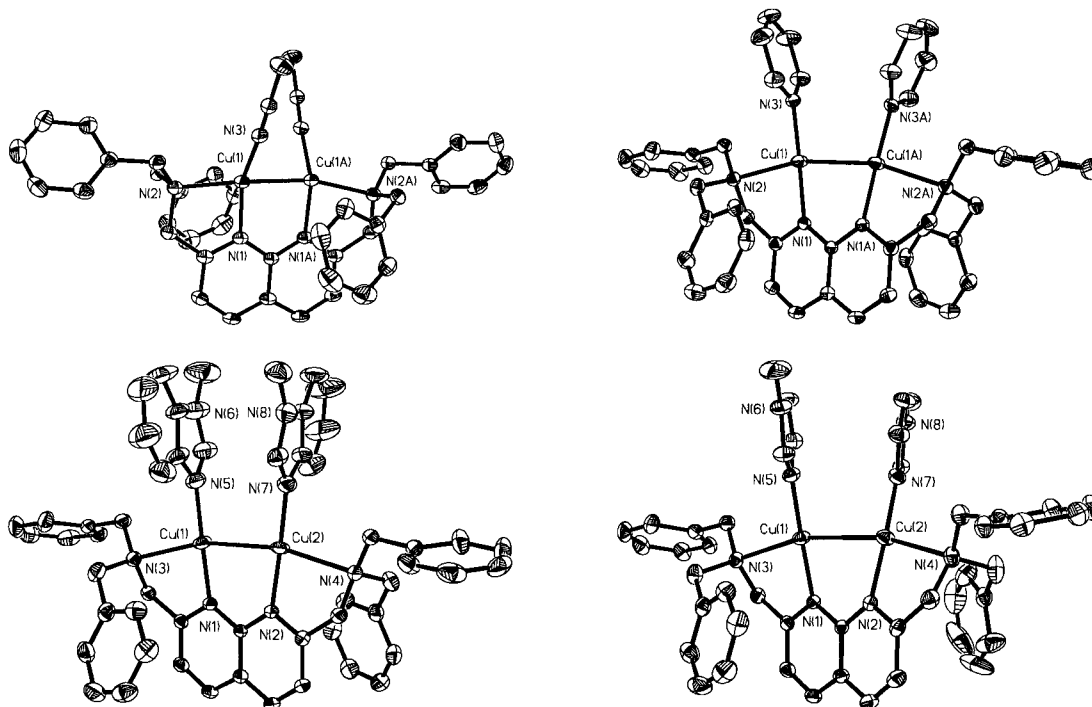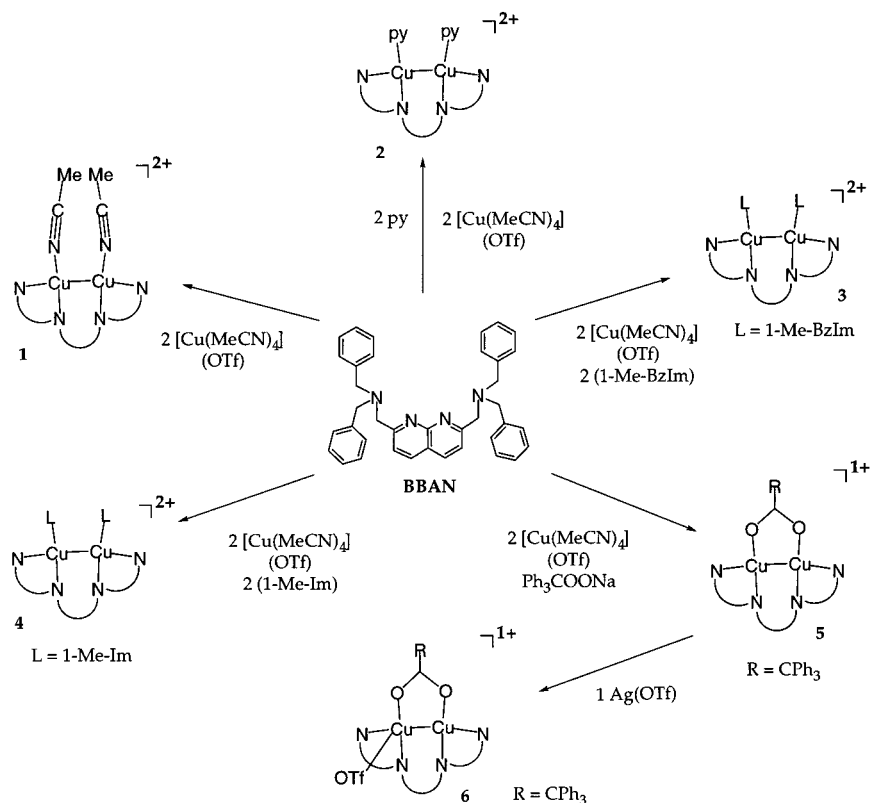
different terminally bound ligands were prepared as illustrated in Scheme 1. Treatment of the ligand BBAN with two equiv of [Cu(CH$_3$CN)$_4$](OTf) in THF gave **1** as a pink solid in high yield (84%). A clear yellow solution was obtained when 2 equiv of pyridine was added to the slurry of **1** in THF. Subsequent crystallization from CH$_2$Cl$_2$/EtO$_2$ afforded complex **2**. Complexes **3−5** were prepared by following same procedure except that **5** was crystallized from pentane/Et$_2$O/benzene. As shown in Figure 2, each copper in [Cu$_2$(BBAN)(MeCN)$_2$](OTf)$_2$ (**1**) is ligated to one nitrogen atom of 1,8-naphthyridine, one tertiary amine nitrogen atom and one terminally bound acetonitrile molecule. Each copper has square-planar coordination geometry. A short copper−copper distance of 2.6879(7) Å was observed from the crystal structure. Dicopper(I) complexes **2−5** have structural features very similar to those of **1** (Figures 2 and 3), and selected bond distances and angles for all five complexes are listed in Table 3. The copper−copper distances among complexes **2−4** vary with the different donating strengths of the terminal ligands. The most donating ligand, 1-methylimidazole in **4**, affords the longest copper−copper distance of 2.7328(5) Å, whereas the least donating terminal ligand, pyridine in **2**, affords the shortest copper−copper distance of 2.6574(6) Å (Table 3). The terminal ligand−copper bond distances vary with the reverse trend. The SOMO of a dicopper complex with same geometry has considerable Cu d$_{x^2-y^2}$/Cu d$_{x^2-y^2}$ σ-antibonding character, as revealed from our previous extended Hückel molecular orbital calculations.[18] The extra electron density donated into this antibonding orbital by terminally bound ligands apparently weakens the copper−copper interaction. With a bridging carboxylate group, the copper−copper distance of 2.6151(6) Å in **5** is, not surprisingly, the shortest among all compounds. Interactions involving π−π stacking between terminal aromatic ligands (~3.4 Å) may also contribute to the shortening of copper−copper distances in **2−4** compared to **1**. In the latter, which has a longer copper−copper distance than those in **2** and **3**, such an interaction cannot occur.

Preparation and Structural Characterization of the Mixed-Valence Complex [Cu$_2$(BBAN)(μ-O$_2$CCPh$_3$)(OTf)](OTf) (6). Complex **6** was prepared by one electron oxidation of **5** with 1 equiv of silver(I) triflate in THF (Scheme 1). After the resulting precipitate was filtered off, deep purple crystals of **6** were obtained from pentane/Et$_2$O/CH$_2$Cl$_2$. The crystal structure of **6** is shown in Figure 3, and selected bond distances and angles are listed in Table 3. One copper atom in **6** maintains square-planar coordination geometry. The other copper is five-coordinate with pyramidal geometry and a terminally bound triflate.

Figure 2. ORTEP diagrams of [Cu$_2$(BBAN)(MeCN)$_2$](OTf)$_2$ (**1**), [Cu$_2$(BBAN)(py)$_2$](OTf)$_2$ (**2**), [Cu$_2$(BBAN)(1-Me-BzIm)$_2$](OTf)$_2$ (**3**), and [Cu$_2$-(BBAN)(1-Me-Im)$_2$](OTf)$_2$ (**4**), showing the 40% probability thermal ellipsoids for all non-hydrogen atoms (left to right and top to bottom).

Scheme 1

The copper–copper distance of 2.4500(15) Å is significantly shorter than that in the dicopper(I) compound **5**. The observed asymmetric dicopper coordination is probably a consequence of the sterically bulky BBAN ligand, which prevents simultaneous binding of two terminal triflate ligands.

Physical Properties of the Mixed-Valence Complex [Cu$_2$(BBAN)(μ-O$_2$CCPh$_3$)(OTf)](OTf) (6). The UV–vis spectrum of **6** exhibits an intense peak at 875 nm (ϵ = 3775 M^{-1} cm^{-1}), a peak at 500 nm (ϵ = 1583 M^{-1} cm^{-1}), and two shoulders at 660 nm (ϵ = 1450 M^{-1} cm^{-1}) and 550 nm (ϵ = 1425 M^{-1} cm^{-1}), as shown in Figure 4. The absorption features are close to those observed in class III mixed-valence macrocyclic octaazacryptand complexes. The sharp intense peak at 875 nm is red-shifted by about 140 nm, and the peak at 500 nm is blue-shifted by about 120 nm compared to those of the all-nitrogen octaazacryptand-based compounds.[14−16] The spec-
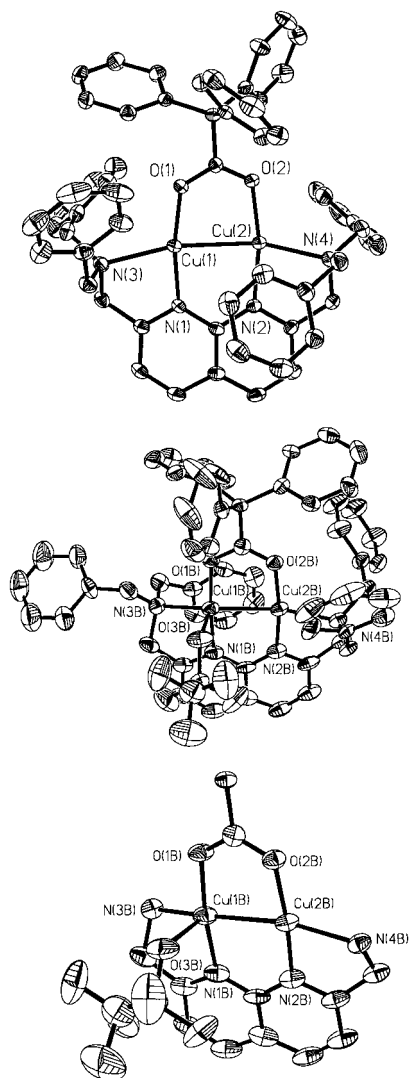
Figure 3. ORTEP diagrams of [Cu$_2$(BBAN)(μ-O$_2$CCPh$_3$)](OTf)$_2$ (**5**), [Cu$_2$(BBAN)(μ-O$_2$CCPh$_3$)(OTf)](OTf) (**6**), and core fragment of **6**, showing the 40% probability thermal ellipsoids for all non-hydrogen atoms (top to bottom).

trum of **6** compares well with those of the XDK-based class III mixed-valence complexes, except that the peak around 875 nm is much more intense.[18] The appearance of several shoulders in the spectrum of **6** is not fully understood.

The X-band EPR spectrum of **6** was measured in a frozen solution (2-methyltetrahydrofuran glass) at 77 and 4 K (Figure 5). A seven-line hyperfine coupling pattern on the lowest field component can be clearly distinguished. The two higher field components have overlapping features. The seven-line pattern arises from the coupling of the unpaired electron to a pair of $I = 3/2$ copper nuclei. The pattern of the spectrum is very similar to that measured at 4 K (Figure 5). The temperature-independent behavior confirms the fully delocalized class III nature of compound **6**. The spectrum taken at 77 K was simulated to afford g values and copper hyperfine coupling constants of $g_1 = 2.002$, $g_2 = 2.100$, $g_3 = 2.222$, $A_1^{Cu} = 30$ G, $A_2^{Cu} = 60$ G, and $A_3^{Cu} = 143$ G. These values resemble those obtained from bis(carboxylate) model complexes (Table 1). These two types of complexes share similar structural features. Complex **6** can be viewed as a member of the bis(carboxylate) mixed-valence family except that one such bridging group is replaced by a masked carboxylate, the neutral bridging 1,8-naphthyridine unit of BBAN.

Table 3. Selected Bond Lengths (Å) and Angles (deg)^a

	bond lengths		bond angles	
1	Cu(1)···Cu(1A)	2.6879(7)	N(2)−Cu(1)−Cu(1A)	150.93(6)
	Cu(1)−N(1)	1.955(2)	N(1)−Cu(1)−N(3)	157.25(10)
	Cu(1)−N(2)	2.187(2)	N(2)−Cu(1)−N(3)	111.70(9)
	Cu(1)−N(3)	1.867(2)	N(1)−Cu(1)−Cu(1A)	84.04(6)
2	Cu(1)···Cu(1A)	2.6574(7)	N(1)−Cu(1)−Cu(1A)	164.04(4)
	Cu(1)−N(1)	1.9542(17)	N(1)−Cu(1)−N(3)	175.85(7)
	Cu(1)−N(2)	2.3583(16)	N(2)−Cu(1)−N(3)	99.09(6)
	Cu(1)−N(3)	1.9308(17)	N(1)−Cu(1)−Cu(1A)	84.06(5)
3	Cu(1)···Cu(2)	2.6716(7)	N(3)−Cu(1)−Cu(2)	161.99(8)
	Cu(1)−N(1)	1.944(3)	N(4)−Cu(2)−Cu(1)	163.45(8)
	Cu(1)−N(3)	2.349(3)	N(1)−Cu(1)−N(5)	178.72(17)
	Cu(1)−N(5)	1.928(4)	N(2)−Cu(2)−N(7)	176.08(17)
	Cu(2)−N(2)	1.937(3)		
	Cu(2)−N(4)	2.403(3)		
	Cu(2)−N(7)	1.923(4)		
4	Cu(1)···Cu(2)	2.7328(5)	N(3)−Cu(1)−Cu(2)	163.61(5)
	Cu(1)−N(1)	1.9483(19)	N(4)−Cu(2)−Cu(1)	162.19(6)
	Cu(1)−N(3)	2.379(2)	N(1)−Cu(1)−N(5)	174.24(9)
	Cu(1)−N(5)	1.909(2)	N(2)−Cu(2)−N(7)	169.98(10)
	Cu(2)−N(2)	1.946(2)		
	Cu(2)−N(4)	2.352(2)		
	Cu(2)−N(7)	1.909(2)		
5	Cu(1)···Cu(2)	2.6151(6)	N(3)−Cu(1)−Cu(2)	167.55(7)
	Cu(1)−N(1)	1.929(3)	N(4)−Cu(2)−Cu(1)	158.12(10)
	Cu(1)−N(3)	2.303(3)	N(1)−Cu(1)−O(1)	169.42(11)
	Cu(1)−O(1)	1.891(2)	N(2)−Cu(2)−O(2)	168.48(11)
	Cu(2)−N(2)	1.976(3)		
	Cu(2)−N(4)	2.221(3)		
	Cu(2)−O(2)	1.948(2)		
6	Cu(1B)···Cu(2B)	2.4493(14)	N(3B)−Cu(1B)−Cu(2B)	162.8(2)
	Cu(1B)−N(1B)	1.911(7)	N(4B)−Cu(2B)−Cu(1B)	168.98(18)
	Cu(1B)−N(3B)	2.090(6)	N(1B)−Cu(1B)−O(1B)	171.8(3)
	Cu(1B)−O(1B)	1.872(5)	N(2B)−Cu(2B)−O(2B)	170.9(3)
	Cu(1B)−O(3B)	2.257(6)	N(1B)−Cu(1B)−O(3B)	96.1(2)
	Cu(2B)−N(2B)	1.907(7)	O(1B)−Cu(1B)−O(3B)	91.3(2)
	Cu(2B)−N(4B)	2.113(6)	Cu(2B)−Cu(1B)−O(3B)	95.23(17)
	Cu(2B)−O(2B)	1.883(5)		

^{a} Numbers in parentheses are estimated standard deviations of the last significant figure. Atoms are labeled as indicated in Figures 2 and 3.
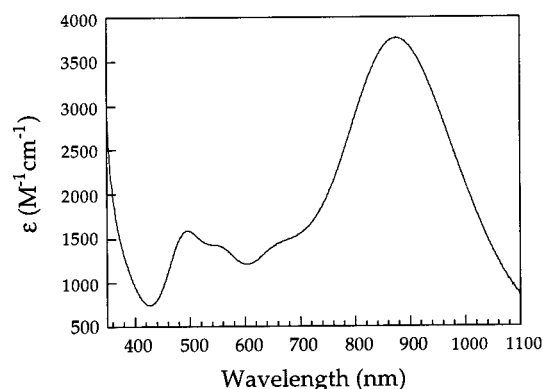

Figure 4. UV−vis spectrum of [Cu$_2$(BBAN)(μ-O$_2$CCPh$_3$)(OTf)](OTf) (**6**), 0.4 mM in THF.

Electrochemistry. The cyclic voltammograms of compounds **1**−**5** were recorded in tetrahydrofuran. No reversible redox waves were observed for **1**−**4**. Attempts to oxidize chemically complexes **1**−**4** with 1 equiv of silver(I) triflate in THF and CH$_2$Cl$_2$ did not yield purple solutions characteristic of a mixed-valence dicopper(I,II) species. A mixed-valence dicopper(I,II) complex apparently cannot be stabilized with the ligand donor sets in these compounds. A chemically reversible ($I_{pa}/I_{pc} \sim 1$) and electrochemically quasireversible ($\Delta E_p = 150$ mV, scan rate = 75 mV/s) redox wave was observed for **5**, however, with $E_{1/2} = -25$ mV vs Cp$_2$Fe$^+$/Cp$_2$Fe (Figure 6). This $E_{1/2}$ value falls in the positive end of the range characteristic of blue copper
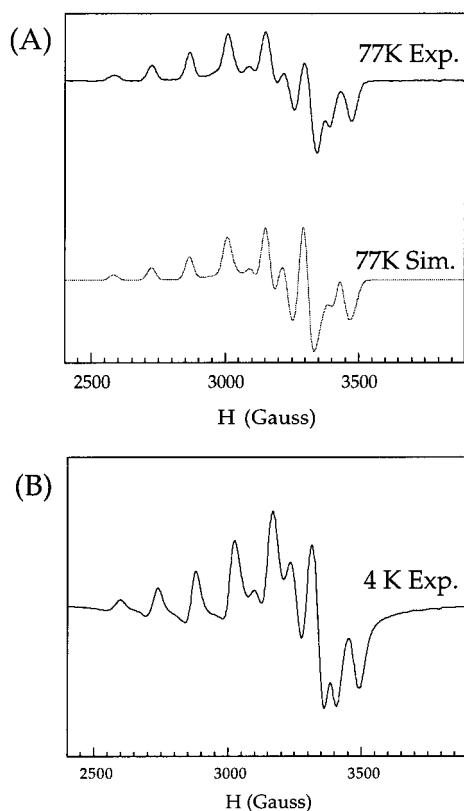
Figure 5. X-band EPR spectra for [Cu₂(BBAN)(μ-O₂CCPh₃)(OTf)]-(OTf) (**6**): (A) frozen solution (2 mM in 2-Me-THF) at 77 K, experimental and simulated data; (B) frozen solution (2 mM in 2-Me-THF) data at 4 K.
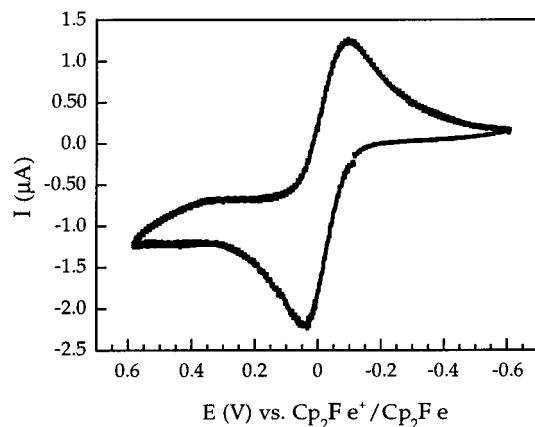

Figure 6. Cyclic voltammogram of 2 mM Cu₂(BBAN)(μ-O₂CCPh₃)]-(OTf) (**5**) in THF with 0.5 M (Bu₄N)(PF₆) as supporting electrolyte and a scan rate of 75 mV/s.

proteins, ∼+200 to +800 mV vs NHE or ∼ −600 to 0 mV vs Cp₂Fe⁺/Cp₂Fe in THF.[30,31]

The $E_{1/2}$ value of the previously reported macrocyclic octaazacryptand complexes is +310 mV vs Ag/AgCl in DMF, which corresponds to −206 mV vs Cp₂Fe⁺/Cp₂Fe in THF.[18] With the anionic dicarboxylate ligand XDK, the $E_{1/2}$ value of the mixed-valence compound is −218 mV vs Cp₂Fe⁺/Cp₂Fe in THF. The anionic bis(carboxylate) ligand does not seem to decrease the redox potential of the Cu^II Cu^I/Cu^I Cu^I couple compared to the all-nitrogen octaazacryptand ligands. This result is

attributed to stabilization of the two-coordinate, linear dicopper(I) geometry by the convergent bis(carboxylate) XDK ligand. Although not reversible, a potential at $E_{1/2}$ = +350 mV vs SCE in MeOH was reported for the bis(μ-thiolato)dicopper-(I,II) compound. This potential can be scaled to approximately −210 mV vs Cp₂Fe⁺/Cp₂Fe in THF. The redox potentials (−206, −218, and −210 mV), observed in these earlier model compounds with completely different ligand environments, are thus very close to each other.

Complex **5** on the other hand exhibits a very different redox potential compared to the model complexes prepared so far. The $E_{1/2}$ value of **5,** which contains only a single anionic carboxylate bridge, is almost 200 mV higher than that of the XDK complexes. The change of one carboxylate in mixed-valence XDK complexes to the 1,8-naphthyridine nitrogen analogue shifts the redox potential by +200 mV. The presence of one additional anionic carboxylate in the XDK complexes thus renders the dicopper(I) core easier to oxidize. The Cu_A site has a redox potential of approximately +240 mV vs NHE, corresponding to −560 mV vs Cp₂Fe⁺/Cp₂Fe in THF.[30−32] With a pair of very donating anionic thiolate bridges and two His ligands, Cu_A site has a low redox potential compared to all model compounds, since addition of an anionic carboxylate ligand can cause a −200 mV change of the redox potential in these similar types of systems.

The neutral all-nitrogen ligands in **1−4** cannot stabilize the mixed-valence Cu^I Cu^II state. In fact, the mixed-valence dicopper(I,II) octaazacryptand complexes are not stable in organic solvents and decay upon standing.[15] It appears that anionic ligands are preferred to stabilize the mixed-valence dicopper(I,II) core. Two thiolate groups are used in nature, and carboxylate groups are utilized in **6** and in the XDK dicopper complexes.

Conclusions

A family of dicopper(I) complexes with short copper−copper distances have been assembled by using a 1,8-naphthyridine-based dinucleating ligand BBAN and different terminal ligands. Chemical and electrochemical oxidation studies of these complexes revealed that, with neutral nitrogen-donor terminal ligands, the mixed-valence dicopper(I,II) analogues could not be stabilized. A fully delocalized mixed-valence dicopper(I,II) complex was prepared by chemically oxidizing a carboxylate-bridged dicopper(I) complex. Frozen solution EPR studies demonstrate the fully delocalized nature of this complex down to 4 K. A cyclic voltammetric study indicated a reversible redox wave with an $E_{1/2}$ value that is +200 mV compared to those of previous model compounds. The $E_{1/2}$ values of the mono-(carboxylate) compound prepared in this work and the structurally very similar bis(carboxylate) XDK compounds reveal the contribution from an anionic carboxylate group to the redox potential of the mixed-valence system to be ∼ −200 mV. Anionic ligands are important factors in stabilizing the mixed-valence state and controlling the redox potential.

Supporting Information Available: X-ray crystallographic files, in CIF format, for complexes **1−6**. This material is available free of charge via the Internet at http://pubs.acs.org.

(30) Reinhammar, B. R. M. *Biochim. Biophys. Acta* **1972**, *275*, 245−259.
(31) Tronson, D. A.; Ritchie, G. A. F.; Nicholas, D. J. D. *Biochim. Biophys. Acta* **1973**, *310*, 331−343.

(32) Immoos, C.; Hill, M. G.; Sanders, D.; Fee, J. A.; Slutter, C. E.; Richards, J. H.; Gray, H. B. *JBIC* **1996**, *1*, 529−531.